

Area Light Sources for Real-Time Graphics

John M. Snyder

March 6, 1996

Technical Report
MSR-TR-96-11

Microsoft Research
Advanced Technology Division
Microsoft Corporation
One Microsoft Way
Redmond, WA 98052

Abstract

In an effort to extend the sorts of lighting models used in real-time computer graphics, this paper presents several area light source models, including Lambertian and Phong illumination from constant and cosine-falloff hemispherical light sources, constant subhemispherical light sources, and constant polygonal light sources. The subhemispherical lighting model can also be used to represent illumination from finite-distance spherical light sources. The models are not unduly more expensive than the simple point light source models, and are capable of real-time evaluation.

1 Introduction

Finite area light sources can make a big difference in the realism of synthetic imagery. New results [Arvo95] make it possible to analytically compute the illumination at a point from area light sources for simple kinds of lighting models, including perfect Lambertian reflectance, and Phong model specular reflectance. This paper explores some of these results as well as some new, special cases and extensions that are particularly easy to compute (e.g., infinite hemispherical light sources, and a simpler specular reflectance model). The computations are simple enough to be implemented as part of the standard graphics illumination model present in every rendering API.

In addition to added realism, there are two more benefits of replacing the traditional point light source models with area light sources. First, area light sources are softer, tending to reduce the variation of surface intensity. This is true at both the specular highlight falloff region and at the terminator line for Lambertian models. Real-time graphics systems typically sample the illumination at the vertices of each polygon and linearly interpolate the shading function between the vertices. High-frequency, nonlinear variation of the surface shading thus requires finely tessellated polygons. Using area light sources reduces this variation and allows larger polygons to be rendered with an acceptable degree of fidelity to the pixel-by-pixel shading variation.

Second, area light sources suffer less from the problem of highlight burnout, in which regions very near to the precise peak of the highlight are clipped to the maximum intensity, thereby becoming regions of constant color with attendant Mach bands. Area light sources tend to create more gradation within these burnout regions. This is not exactly a contradiction of the statements of the previous paragraph: area light sources both soften (i.e., reduce variation) in the near-peak specular falloff region, and add variation in the formerly constant peak regions.

A summary of the main results of this paper is contained in Section 4.

2 Lambertian Lighting

We first consider perhaps the simplest form of lighting model, Lambert's law, in which incident light is scattered so as to appear equally bright from all directions. Given a point P on a surface with unit-length normal N , Lambert's law states that the output intensity, I , is equal in any direction and given by

$$I \equiv \frac{1}{I_{\text{norm}}} \int_{H(N)} F(p) (p \cdot N) dA(p) \quad (1)$$

where $H(N)$ is a unit-radius hemisphere around N , p is a point on this hemisphere representing the incident direction, F is the incident radiance as a function of incident direction, and dA is the differential area of the surface element at p . I_{norm} is a factor that normalizes the BRDF; i.e.,

$$I_{\text{norm}} \equiv \int_{H(N)} (p \cdot N) dA(p) = \pi.$$

We will show that $I_{\text{norm}} = \pi$ in the next section.

The following sections compute I analytically for various light sources; that is, for various incident radiance distributions $F(p)$.

2.1 Infinite Hemispherical Light Sources

An infinite hemispherical light source is defined by a light direction L which represents the "top" of the hemisphere. An arbitrary direction D receives light only if $D \cdot L \geq 0$. Such a model ignores the location of the point to be illuminated (P); only the normal at the point (N) matters. For example, a scene may be lighted by an infinite hemispherical light source whose direction corresponds to the zenith, a model that is a reasonable approximation to sky illumination [Nishita86]. Within the

general category of infinite hemispherical light sources, various subtypes can be defined that apply different weighting to the incident radiances over the hemisphere. The next sections define analytic shading functions for both constant-weighted and cosine-weighted hemispherical light sources. These can be combined (Section 2.1.3) to produce a reasonable simulation of illumination from an overcast sky.

Subsequent derivations make use of the following hemispherical parameterization. This parameterization assumes that the coordinate system has been arranged so that N is transformed to the z -axis, and the perpendicular projection of L onto N is mapped to the negative x -axis. The hemisphere around N is then given by

$$p(\theta, \phi) \equiv \begin{pmatrix} \cos \theta \sin \phi \\ -\cos \phi \\ \sin \theta \sin \phi \end{pmatrix}$$

where $\theta \in [0, \pi]$ and $\phi \in [0, \pi]$. The angle between N and L is denoted by ω , where $\omega \in [0, \pi]$. Figure 1 illustrates this hemispherical parameterization.

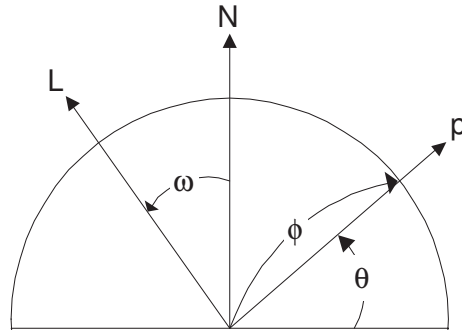


Figure 1: Hemispherical parameterization: A point on the hemisphere is given by $p(\theta, \phi)$ where θ parameterizes the angle in the plane of N and L , and ϕ parameterizes the angle perpendicular to this plane. ω is the angle between L and N .

Using this parameterization, we have

$$\begin{aligned} I_{\text{norm}} &= \int_0^\pi d\theta \int_0^\pi d\phi F(\theta, \phi) \sin \theta \sin^2 \phi \\ &= \pi. \end{aligned}$$

This is because the differential area is given by

$$dA = \sin \phi d\theta d\phi$$

and because the Lambert's law dot product reduces to

$$p \cdot N = \sin \theta \sin \phi$$

in the transformed coordinate system. Thus

$$I_{\text{hemi}}(\omega) \equiv \frac{1}{\pi} \int_\omega^\pi d\theta \int_0^\pi d\phi F(\theta, \phi) \sin \theta \sin^2 \phi. \quad (2)$$

The limits on θ are $[\omega, \pi]$ since there is no incident radiance except in the hemisphere about L , and the hemisphere about N intersects the hemisphere about L in the range $\theta = \omega$ to $\theta = \pi$ (refer to Figure 1). The integration limits on ϕ are $[0, \pi]$, just as in the original hemisphere.

2.1.1 Constant-Weighted

In the constant-weighted hemisphere case, we have

$$F(\theta, \phi) \equiv \begin{cases} 0, & \text{if } L \cdot p(\theta, \phi) < 0 \\ 1, & \text{otherwise.} \end{cases}$$

Equation 2 becomes

$$I_{\text{hemi-const}}(\omega) = \frac{1}{\pi} \int_{\omega}^{\pi} d\theta \int_0^{\pi} d\phi \sin \theta \sin^2 \phi$$

which reduces to

$$\begin{aligned} I_{\text{hemi-const}} &= \frac{1}{\pi} \left[\frac{\phi}{2} - \frac{\sin 2\phi}{4} \right] \Big|_0^{\pi} \left[-\cos \theta \right] \Big|_{\omega}^{\pi} \\ &= \frac{1}{2}(1 + \cos \omega). \end{aligned} \quad (3)$$

Converting back into the global coordinate system, we have

$$I_{\text{hemi-const}}(N, L) = \frac{1}{2}(1 + N \cdot L) \quad (4)$$

2.1.2 Cosine-Weighted

In the cosine-weighted hemisphere case, we have

$$F(\theta, \phi) \equiv L \cdot p(\theta, \phi)$$

where L expressed in the special coordinate is given by

$$L \equiv \begin{pmatrix} \cos(\frac{\pi}{2} + \omega) \\ 0 \\ \sin(\frac{\pi}{2} + \omega) \end{pmatrix} = \begin{pmatrix} -\sin \omega \\ 0 \\ \cos \omega \end{pmatrix}.$$

Equation 2 becomes

$$I_{\text{hemi-cos}}(\omega) = \frac{1}{\pi} \int_{\omega}^{\pi} d\theta \int_0^{\pi} d\phi [-\sin \omega \cos \theta \sin \phi + \cos \omega \sin \theta \sin \phi] \sin \theta \sin^2 \phi$$

which reduces to

$$\begin{aligned} I_{\text{hemi-cos}}(\omega) &= \frac{1}{\pi} \int_{\omega}^{\pi} \int_0^{\pi} \sin^3 \phi [-\sin \omega \sin \theta \cos \theta + \cos \omega \sin^2 \theta] d\theta d\phi \\ &= \frac{1}{\pi} \left[-\frac{1}{3} \cos \phi (\sin^2 \phi + 2) \right] \Big|_0^{\pi} \left[-\sin \omega \frac{\sin^2 \theta}{2} + \cos \omega \left(\frac{\theta}{2} - \frac{1}{4} \sin 2\theta \right) \right] \Big|_{\omega}^{\pi} \\ &= \frac{4}{3\pi} \left(\frac{\sin^3 \omega}{2} + \cos \omega \left(\frac{\pi}{2} - \frac{\omega}{2} + \frac{1}{4} \sin 2\omega \right) \right) \\ &= \frac{2}{3\pi} (\sin^3 \omega + \cos \omega (\pi - \omega + \sin \omega \cos \omega)). \end{aligned} \quad (5)$$

Converting back into the global coordinate system is easily accomplished since

$$\begin{aligned} \cos \omega &= N \cdot L \\ \sin \omega &= \sqrt{1 - (N \cdot L)^2} \\ \omega &= \cos^{-1}(N \cdot L) \end{aligned}$$

Note that this light source type requires evaluation of the inverse cosine function to calculate the output intensity.

2.1.3 Combining Weights: The CIE Sky Model

The above two weighting functions can be combined to yield illumination from an infinite hemispherical light source whose incident radiance is a linear combination of constant and cosine-weighted functions. More precisely, we define the output intensity as $I_{\text{hemi-sum}}$, given by

$$I_{\text{hemi-sum}}(\omega, \alpha, \beta) \equiv \alpha I_{\text{hemi-const}}(\omega) + \beta I_{\text{hemi-cos}}(\omega).$$

For example, The CIE Standard sky luminance function [Nishita86] can be used as a model for illumination from overcast skies. This model weights the radiance function over the hemisphere using

$$I_{\text{hemi-sum}}(\omega, \frac{C}{3}, \frac{2C}{3})$$

where C is the luminance at the sky zenith (i.e., in the direction L).

2.2 Sub-Hemispherical Light Sources

Similar derivations can be used to construct the analytic shading function due to a finite spherical light source that is a perfectly diffuse emitter, or due to an infinite light source that subtends a fixed angle of less than π . We define a *sub-hemispherical light source*, a generalization of the hemispherical light source introduced in Section 2.1. Such a light source is defined with a direction L that points toward the center of the light source, and an angle $\sigma \in [0, \pi/2]$, representing the maximum angle an incident direction can make with L . That is, an arbitrary direction D receives light only if $D \cdot L \geq \cos \sigma$. The hemispherical case considered before is thus a specialization, for which $\sigma = \pi/2$.

It can be shown (Section A) that Lambertian lighting due to such a light source has the following analytic form:

$$I_{\text{hemi-sub}}(\omega, \sigma) \equiv \frac{1}{\pi} \begin{cases} \pi \cos \omega \sin^2 \sigma, & \omega \in [0, \frac{\pi}{2} - \sigma] \\ \pi \cos \omega \sin^2 \sigma + G(\omega, \sigma, \gamma) - H(\omega, \sigma, \gamma), & \omega \in [\frac{\pi}{2} - \sigma, \frac{\pi}{2}] \\ G(\omega, \sigma, \gamma) + H(\omega, \sigma, \gamma), & \omega \in [\frac{\pi}{2}, \frac{\pi}{2} + \sigma] \\ 0, & \omega \in [\frac{\pi}{2} + \sigma, \pi] \end{cases} \quad (6)$$

where

$$\gamma \equiv \sin^{-1} \left(\frac{\cos \sigma}{\sin \omega} \right),$$

$$G(\omega, \sigma, \gamma) \equiv -2 \sin \omega \cos \sigma \cos \gamma + \frac{\pi}{2} - \gamma + \sin \gamma \cos \gamma,$$

and

$$H(\omega, \sigma, \gamma) \equiv \cos \omega \left[\cos \gamma \sqrt{\sin^2 \sigma - \cos^2 \gamma} + \sin^2 \sigma \sin^{-1} \left(\frac{\cos \gamma}{\sin \sigma} \right) \right].$$

As in the previous section, ω is the angle between N and L . We also note that trigonometric evaluations can be avoided by observing

$$\begin{aligned} \sin \gamma &= \frac{\cos \sigma}{\sin \omega} \\ \cos \gamma &= \sqrt{1 - \sin^2 \gamma} \end{aligned}$$

Figure 2 illustrates the sub-hemispherical model for various values of σ . Note that $I_{\text{hemi-sub}}$ is a generalization of $I_{\text{hemi-const}}$ from Section 2.1.1, where

$$I_{\text{hemi-const}}(\omega) = I_{\text{hemi-sub}}(\omega, \frac{\pi}{2}).$$

In the case of an infinite sub-hemispherical light source, σ is a constant for all points (P, N) to be illuminated. In this case, the quantities $\cos \sigma$ and $\sin \sigma$ should be computed as a pre-preprocessing step and stored. As in the case for infinite hemispherical light sources, the location of the point in space, P , is ignored.

The sub-hemispherical model can also be used to model illumination from a finite spherical light source. Given the position of the light source, P_L , and its radius, r , we can compute the angle subtended at a point to be illuminated, P , via

$$\sigma = \sin^{-1} \left(\frac{r}{\|P - P_L\|} \right) \quad (7)$$

i.e.,

$$\begin{aligned} \sin \sigma &= \frac{r}{\|P - P_L\|} \\ \cos \sigma &= \sqrt{1 - \sin^2 \sigma}. \end{aligned}$$

In this case, both σ and ω vary as (P, N) varies, for the same light source.

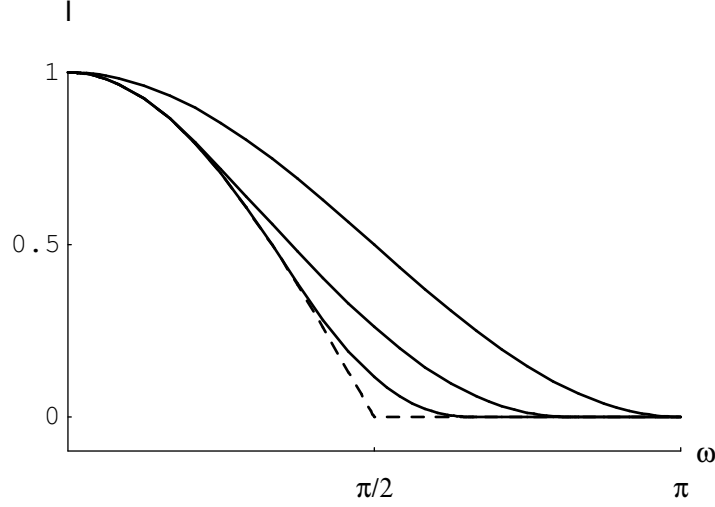


Figure 2: Normalized Sub-Hemispherical Illumination: The relation of the “normalized” shading function to ω is plotted for values of $\sigma = \frac{\pi}{6}$, $\frac{\pi}{3}$, and $\frac{\pi}{2}$. Normalization means dividing by $\sin^2 \sigma$ so as to return a maximum result (at $\omega = 0$) of 1. The dashed line represents the point light source model $\max(0, \cos \omega)$. The sub-hemispherical model essentially produces a “fillet” over the smoothness discontinuity in the point light source curve, where the smoothness of the fillet increases with increasing σ .

Approximating the sub-hemispherical model The computations required by Equation 6 are fairly complex, including two inverse trigonometric operations to calculate γ and $H(\omega, \sigma, \gamma)$. Computations can be reduced by approximating the “fillet” region of $I_{\text{hemi-sub}}$ (i.e., $\omega \in [\frac{\pi}{2} - \sigma, \frac{\pi}{2} + \sigma]$) as a cubic curve. At one endpoint of this segment, $\omega = \frac{\pi}{2} - \sigma$,

$$I_{\text{hemi-sub}}\left(\frac{\pi}{2} - \sigma\right) = \cos\left(\frac{\pi}{2} - \sigma\right) \sin^2 \sigma = \sin^3 \sigma$$

and

$$\frac{dI_{\text{hemi-sub}}}{d\omega}\left(\frac{\pi}{2} - \sigma\right) = -\sin\left(\frac{\pi}{2} - \sigma\right) \sin^2 \sigma = -\cos \sigma \sin^2 \sigma.$$

At the other endpoint, $\omega = \frac{\pi}{2} + \sigma$,

$$I_{\text{hemi-sub}}\left(\frac{\pi}{2} + \sigma\right) = 0$$

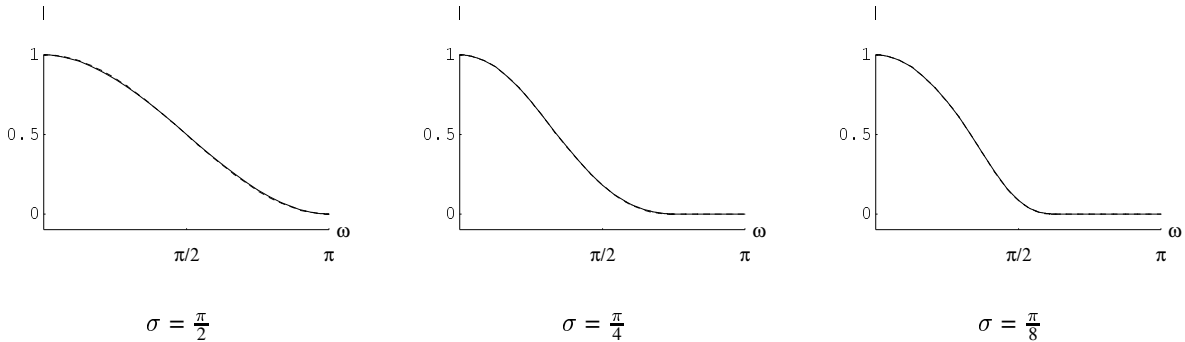


Figure 3: Approximate Sub-hemispherical Illumination: The three plots show the accuracy with which the two-segment hermite interpolation approximates the sub-hemispherical Lambertian model. The dashed line represents the actual model; the solid is the approximate model. The plots represent normalized intensity vs. ω for $\sigma = \frac{\pi}{2}, \frac{\pi}{4}, \frac{\pi}{8}$.

and

$$\frac{dI_{\text{hemi-sub}}}{d\omega}\left(\frac{\pi}{2} + \sigma\right) = 0.$$

We can therefore use hermite interpolation to construct an approximation to this segment.

Hermite interpolation approximates a function $f(x)$ in an interval by a cubic curve, given its value and the value of its first derivative at the endpoints of the interval. Let the value of the function and its derivatives at the endpoints of the interval $[x_0, x_1]$ be given by

$$f(x_0) = f_0, \quad f(x_1) = f_1, \quad f'(x_0) = f'_0, \quad f'(x_1) = f'_1.$$

For the canonical interval $[0, 1]$, the cubic curve having given endpoints values of

$$g(0) = g_0, \quad g(1) = g_1, \quad g'(0) = g'_0, \quad g'(1) = g'_1.$$

is

$$g(y) \equiv ay^3 + by^2 + cy + d$$

where

$$\begin{aligned} a(g_0, g_1, g'_0, g'_1) &\equiv g'_1 + g'_0 - 2(g_1 - g_0) \\ b(g_0, g_1, g'_0, g'_1) &\equiv 3(g_1 - g_0) - g'_1 - 2g'_0 \\ c(g_0, g_1, g'_0, g'_1) &\equiv g'_0 \\ d(g_0, g_1, g'_0, g'_1) &\equiv g_0. \end{aligned}$$

For an arbitrary interval $[x_0, x_1]$, the transformation

$$y = \frac{x - x_0}{x_1 - x_0}$$

can be made. A cubic curve $h(x) = g(y(x))$ approximating $f(x)$ in $[x_0, x_1]$ can then be defined using the above cubic polynomial for $g(y)$, with the following substitutions for the endpoint conditions:

$$\begin{aligned} g_0 &= f_0 \\ g_1 &= f_1 \\ g'_0 &= (x_1 - x_0)f'_0 \\ g'_1 &= (x_1 - x_0)f'_1. \end{aligned}$$

To increase accuracy, we can break the fillet region into two cubic curves instead of one by introducing another knot at $w = \frac{\pi}{2}$.¹ A piecewise cubic curve is then defined using hermite interpolation over the two intervals $[\frac{\pi}{2} - \sigma, \frac{\pi}{2}]$ and $[\frac{\pi}{2}, \frac{\pi}{2} + \sigma]$. The values of the intensity function and its derivative with respect to ω at $\omega = \frac{\pi}{2}$ are given by

$$I_{\text{hemi-sub}}\left(\frac{\pi}{2}\right) = \frac{1}{\pi}(\sigma - \cos \sigma \sin \sigma)$$

and

$$\frac{dI_{\text{hemi-sub}}}{d\omega}\left(\frac{\pi}{2}\right) = -\frac{1}{2} \sin^2 \sigma.$$

Figure 3 shows the results of the two-segment hermite approximation.

2.3 Polygonal Light Sources

Illumination from a uniformly bright (perfectly diffuse) polygonal light source can be analytically integrated; a result first achieved by Lambert in 1760. The result is summarized in [Arvo94], but is repeated here for completeness. The polygonal light source is represented as a collection of m vertices V_1, V_2, \dots, V_m . The output intensity is given by

$$I_{\text{poly}} \equiv \frac{1}{2\pi} \sum_{i=1}^m \Theta_i(P) (\Gamma_i(P) \cdot N) \quad (8)$$

¹This is especially important for large values of σ , since the fillet region becomes larger as $\sigma \rightarrow \frac{\pi}{2}$, becoming the entire curve at $\frac{\pi}{2}$. A single hermite curve is a fairly coarse approximation to $I_{\text{hemi-sub}}$ in this case.

where Θ_i is the angle subtended by the edge from V_i to V_{i+1} , and Γ_i is the “edge normal”. More precisely,

$$\Theta_i(P) \equiv \cos^{-1} \left(\frac{V_i - P}{\|V_i - P\|} \cdot \frac{V_{i+1} - P}{\|V_{i+1} - P\|} \right)$$

and

$$\Gamma_i(P) \equiv \frac{(V_i - P) \times (V_{i+1} - P)}{\|(V_i - P) \times (V_{i+1} - P)\|}$$

where $V_{m+1} = V_1$.

The above expression assumes that the light source is entirely within the hemisphere around N at P . If not, then the light source must be restricted to this hemisphere. This is easily accomplished by clipping the light source polygon to the plane containing P perpendicular to N ; i.e., the plane of points Q for which

$$(Q - P) \cdot N = 0.$$

The set of vertices resulting from clipping the light source polygon to this plane can then be used in Equation 8.

3 Non-Lambertian Lighting

This section considers a simple specular lighting model, the Phong power-law model, in which the output intensity in the viewing direction V is given by

$$I \equiv \frac{1}{I_{\text{norm-Phong}}} \int_{H(R)} F(p) (p \cdot R)^n dA(p). \quad (9)$$

R is the reflection direction, given by reflecting the viewing direction V through the normal N :

$$R \equiv \frac{2N(V \cdot N) - V}{\|2N(V \cdot N) - V\|}.$$

The integral exponent n controls the shininess of the surface; larger exponents yield shinier surfaces. As in the Lambertian case (Equation 1), $H(R)$ is a unit-radius hemisphere (but around around R rather than N), p is a point on this hemisphere representing the incident direction, F is the incident radiance as a function of incident direction, and dA is the differential area of the surface element at p . $I_{\text{norm-Phong}}$ is the normalization factor, given by

$$I_{\text{norm-Phong}} \equiv \int_{H(R)} (p \cdot R)^n dA(p) = \frac{2\pi}{n+1} \quad (10)$$

and will be derived later.

We note that this model is different from the specular models used in both OpenGL model and in [Arvo95], in that different expressions are substituted for $(p \cdot R)^n$. For OpenGL, the power law relation is given by $(p \cdot H)^n$, where H , the “halfway vector”, is given by

$$H \equiv \frac{V + p}{\|V + p\|}.$$

Arvo uses yet another integrand, given by

$$(p \cdot R)^n (p \cdot N).$$

The main difference of these two models from Equation 9 is that the specular intensity falls off as the angle of the plane formed by V and p becomes perpendicular to N . The OpenGL model is difficult to integrate analytically. Arvo’s model is also more difficult to integrate, in that the domain of integration becomes the intersection of the two hemispheres around N and R .

3.1 Phong Illumination from Infinite Hemispherical Light Sources

As in Section 2.1, we first consider lighting from a hemispherical light source. For a constant-weighted light field, using the same spherical parameterization as in Section 2.1, Equation 9 reduces to

$$I_{\text{hemi-const-Phong}}(\omega, n) = \frac{1}{I_{\text{norm-Phong}}(n)} \int_{\omega} d\theta \int_0^{\pi} d\phi (\sin \theta \sin \phi)^n \sin \phi. \quad (11)$$

Similarly, for a cosine-weighted light field, Equation 9 reduces to

$$I_{\text{hemi-cos-Phong}}(\omega, n) = \frac{1}{I_{\text{norm-Phong}}(n)} \int_{\omega}^{\pi} d\theta \int_0^{\pi} d\phi (\sin \theta \sin \phi)^n \sin^2 \phi [-\sin \omega \cos \theta + \cos \omega \sin \theta]. \quad (12)$$

In this case, ω is the angle between the hemispherical direction L with the reflection direction R rather than the normal direction N ; i.e.,

$$\omega = \cos^{-1}(R \cdot L).$$

The normalization factor is given by

$$I_{\text{norm-Phong}}(n) = \int_0^{\pi} d\theta \int_0^{\pi} d\phi (\sin \theta \sin \phi)^n \sin \phi.$$

To compute these integrals analytically, we define the *sine-power-integral function*, $S(n, x)$ as

$$S(n, x) \equiv \int_0^x \sin^n \theta d\theta$$

where $n \geq 0$ is an integer, and $x \in \mathbf{R}$. A recurrence relation can be defined that allows computation of S , via

$$S(n, x) = -\frac{1}{n} \sin^{n-1} x \cos x + \frac{n-1}{n} S(n-2, x)$$

with termination cases given by

$$\begin{aligned} S(0, x) &= x \\ S(1, x) &= 1 - \cos x. \end{aligned}$$

We can thus build the recurrence upward to evaluate $S(n, x)$, using the initial value $S(0, x)$ for even n , and $S(1, x)$ for odd n . We also note that for odd n , only the value of $\cos x$ and $\sin x$ are important for evaluating $S(n, x)$. For even n , the value of x itself is also necessary, implying an additional inverse trigonometric evaluation when only $\cos x$ is known. Code for evaluating the sine-power-integral function can be found in Appendix B.

Using the sine-power-integral function, we first find the value of $I_{\text{norm-Phong}}$ as

$$I_{\text{norm-Phong}} = S(n, \pi) S(n+1, \pi).$$

But $S(n, \pi)$ obeys a particularly simple recurrence relation which can be derived from the general formula above, namely

$$S(n, \pi) = \frac{n-1}{n} S(n-2, \pi)$$

with

$$\begin{aligned} S(0, \pi) &= \pi \\ S(1, \pi) &= 2. \end{aligned}$$

From this result, it can easily be proved by induction that

$$S(n, \pi) S(n+1, \pi) = \frac{2\pi}{n+1} \quad (13)$$

the result stated in Equation 10. We also note that

$$\begin{aligned} S(n, 0) &= 0 \\ S(n, \frac{\pi}{2}) &= \frac{1}{2} S(n, \pi) \end{aligned}$$

for any integer $n \geq 0$.

Equations 11 and 12 then reduce to

$$\begin{aligned} I_{\text{hemi-const-Phong}}(\omega, n) &= \frac{1}{S(n+1, \pi) S(n, \pi)} S(n+1, \pi) (S(n, \pi) - S(n, \omega)) \\ &= 1 - \frac{S(n, \omega)}{S(n, \pi)} \end{aligned} \quad (14)$$

$$\begin{aligned} I_{\text{hemi-cos-Phong}}(\omega, n) &= \frac{1}{S(n+1, \pi) S(n, \pi)} S(n+2, \pi) \left[\frac{1}{n+1} \sin^{n+2} \omega + \cos \omega (S(n+1, \pi) - S(n+1, \omega)) \right] \\ &= \frac{(n+1)}{(n+2) S(n+1, \pi)} \left[\frac{1}{n+1} \sin^{n+2} \omega + \cos \omega (S(n+1, \pi) - S(n+1, \omega)) \right] \end{aligned} \quad (15)$$

Note that the constant $S(n, \pi)$ can be evaluated as a pre-processing step and stored with other surface material characteristics to avoid redundant evaluations. From that constant, $S(n+1, \pi)$ can be derived using Equation 13 as

$$S(n+1, \pi) = \frac{2\pi}{(n+1) S(n, \pi)}.$$

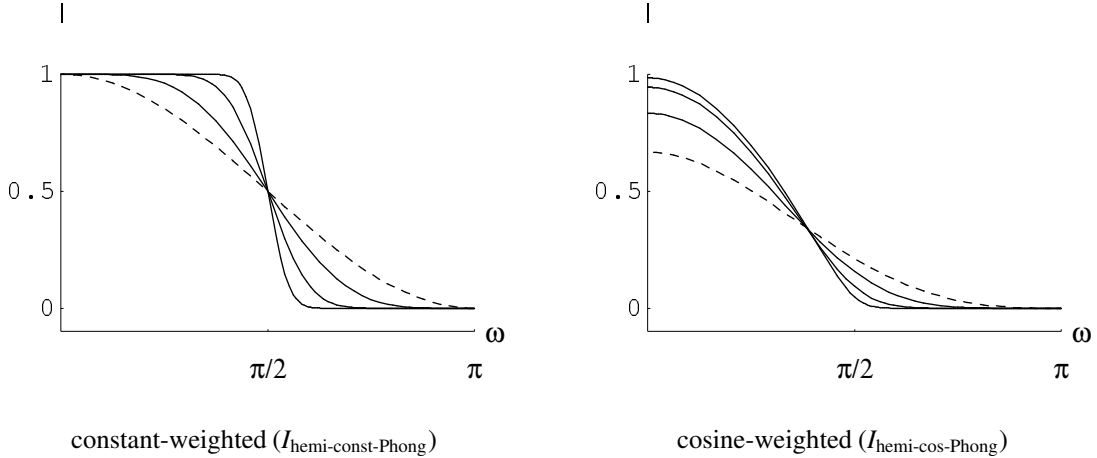


Figure 4: Infinite Hemisphere Phong Illumination: The left side plots constant-weighted model, the right plots the cosine-weighted model, for $n = 1, 4, 16, 64$. The dashed curve represents $n = 1$ on both sides.

Figure 4 compares the infinite hemisphere Phong illumination model (both constant and cosine weighted) for various values of n . Note that $I_{\text{hemi-const-Phong}}$ and $I_{\text{hemi-cos-Phong}}$ are generalizations of the functions $I_{\text{hemi-const}}$ and $I_{\text{hemi-cos}}$, respectively, from Sections 2.1.1 and 2.1.2, where

$$\begin{aligned} I_{\text{hemi-const}}(\omega) &= I_{\text{hemi-const-Phong}}(\omega, 1) \\ I_{\text{hemi-cos}}(\omega) &= I_{\text{hemi-cos-Phong}}(\omega, 1). \end{aligned}$$

3.2 Phong Illumination from Sub-Hemispherical Light Sources

We next analyze the specular lighting model of Equation 9 for sub-hemispherical light sources, as we did in Section 2.2 for the Lambertian model. As in Section 2.2, the incident radiance is described by the function

$$F(p) = \begin{cases} 1, & \text{if } p \cdot L \geq \cos \sigma \\ 0, & \text{otherwise} \end{cases}$$

where L is the direction to the center of the light source, and σ is the size of the light source (i.e., the maximum angle an incident direction can make with L and still hit the light source). This implies Equation 9 is 0 if $\omega \geq \frac{\pi}{2} + \sigma$; i.e.

$$\cos \omega \leq -\sin \sigma$$

since then the light source is entirely outside the hemisphere around R .

To perform the integration, we introduce yet another parameterization of the sphere via

$$p(x, y, z) \equiv \begin{pmatrix} x \\ y \\ z \end{pmatrix}$$

where $x^2 + y^2 + z^2 = 1$. The hemisphere around the reflection direction R is mapped to the hemisphere with $z \geq 0$. Letting $I(n)$ represent the output intensity as a function of the specular exponent n , this parameterization yields

$$I(n) = \int_{\Omega} z^n d\Omega = \int \int_{\Omega_{xy}} z^{n-1} dx dy$$

since

$$dA(p) = \frac{1}{z}$$

for this parameterization. Here Ω represents the part of the hemisphere around R on which the spherical light source projects, and Ω_{xy} the xy projection of this region.

Using Stoke's Theorem (Appendix C), $I(n)$ can be converted to the following series

$$I(n) = \begin{cases} \frac{1}{n+1} \sum_{i=0}^{\frac{n-1}{2}} J(2i+1), & \text{for } n \text{ odd} \\ \frac{1}{n+1} \left[I(0) + \sum_{i=1}^{\frac{n}{2}} J(2i) \right], & \text{for } n \text{ even} \end{cases} \quad (16)$$

where $J(n)$ is a line integral over the boundary of the region Ω , given by

$$J(n) \equiv \int_{\partial\Omega} z^{n-1} (xdy - ydx),$$

and $I(0)$ represents the solid angle subtended by the light source, clipped to the hemisphere around R .

We next consider how to evaluate the boundary integrals $J(n)$. We first note that the boundary of the region Ω is defined by a circular segment around the projection of the spherical light source, denoted C , and (possibly) a segment in the xy plane where the projection of the spherical light source intersects the hemisphere around R , denoted D . But the contribution to $J(n)$ from D is 0 for $n > 1$, since $z = 0$ on this segment, and the integrand contains a factor of z^{n-1} . Thus,

$$J(n) = \begin{cases} \int_C (xdy - ydx) + \int_D (xdy - ydx), & \text{if } n = 1 \\ \int_C z^{n-1} (xdy - ydx), & \text{if } n > 1. \end{cases} \quad (17)$$

To parameterize the boundary C , we transform the light direction L into the simple coordinate system that aligns R with the z axis. Since L makes an angle of ω with R , we use

$$L = \begin{pmatrix} \sin \omega \\ 0 \\ \cos \omega \end{pmatrix}.$$

We also define two perpendicular vectors to L , L_1 and L_2 , so that $\{L_1, L_2, L\}$ form an orthonormal basis of \mathbf{R}^3 , given by

$$L_1 \equiv \begin{pmatrix} \cos \omega \\ 0 \\ -\sin \omega \end{pmatrix}, \quad L_2 \equiv \begin{pmatrix} 0 \\ 1 \\ 0 \end{pmatrix}.$$

Then C may be parameterized by an angle ϕ via

$$C(\phi) = \cos \sigma L + \sin \sigma (\cos \phi L_1 + \sin \phi L_2) \quad (18)$$

since the boundary makes an angle of σ with the central axis L . On this boundary, we then have

$$z = \cos \sigma \cos \omega - \sin \sigma \sin \omega \cos \phi \quad (19)$$

and

$$x dy - y dx = (\sin^2 \sigma \cos \omega + \cos \sigma \sin \sigma \sin \omega \cos \phi) d\phi. \quad (20)$$

Integrating over C in $J(n)$ thus requires integrals of the form

$$F'(a, b, n, \phi_1, \phi_2) \equiv \int_{\phi_1}^{\phi_2} (a + b \cos \phi)^n d\phi$$

and

$$G'(a, b, n, \phi_1, \phi_2) \equiv \int_{\phi_1}^{\phi_2} (a + b \cos \phi)^n \cos \phi d\phi.$$

where

$$\begin{aligned} a &= \cos \sigma \cos \omega \\ b &= -\sin \sigma \sin \omega \end{aligned}$$

and where the integration limits ϕ_1 and ϕ_2 represent the endpoints of C . To simplify the notation, we define F and G with respect to the upper limit of integration only, with a constant lower limit of integration of 0, so that

$$\begin{aligned} F'(a, b, n, \phi_1, \phi_2) &= F(a, b, n, \phi_2) - F(a, b, n, \phi_1) \\ G'(a, b, n, \phi_1, \phi_2) &= G(a, b, n, \phi_2) - G(a, b, n, \phi_1) \end{aligned}$$

The integrals F and G can be computed using the recurrence relations from Appendix D.

To find the integration limits, ϕ_1 and ϕ_2 , two cases arise. In the first, C is entirely within the hemisphere around R , in which case $\phi_1 = 0$ and $\phi_2 = 2\pi$. In the second, we must compute the intersection of C with the $z = 0$ plane, and return the angular range over which the z component of C is non-negative. Solving for $z = 0$ in Equation 19, we have

$$\cos \phi_1 = \cos \phi_2 = -a/b.$$

This also provides a test for whether C is entirely within R 's hemisphere via $|b| \leq |a|$. Since $b \leq 0$,² the segment of the boundary for which $z = a + b \cos \phi \geq 0$ is given by

$$\phi_1 \equiv \begin{cases} 0, & \text{if } -b \leq |a| \\ \cos^{-1}(-a/b), & \text{otherwise} \end{cases} \quad (21)$$

$$\phi_2 \equiv 2\pi - \phi_1 \quad (22)$$

where \cos^{-1} returns a result in $[0, \pi]$. Note also that

$$\begin{aligned} \cos \phi_1 &= \cos \phi_2 = -a/b \\ \sin \phi_1 &= \sqrt{1 - a^2/b^2} \\ \sin \phi_2 &= -\sin \phi_1 \end{aligned}$$

which requires a single inverse trigonometric function evaluation and square root, and no trigonometric function evaluations in order to compute ϕ_1 and ϕ_2 and their sines and cosines.

²This is because $\sigma \leq \frac{\pi}{2}$ and $\omega \leq \pi$.

Since evaluation of $I(n)$ requires summation of a series of terms of $J(i)$, which can be evaluated using a recurrence formula, it is efficient to compute the sum over $J(i)$ as the recurrence is computed. We therefore define the series functions F_{sum} and G_{sum} using

$$F_{\text{sum}}(a, b, n, \phi) \equiv \begin{cases} \sum_{i=0}^{\frac{n-1}{2}} F(a, b, 2i+1, \phi), & \text{if } n \text{ odd} \\ \sum_{i=0}^{\frac{n}{2}} F(a, b, 2i, \phi), & \text{if } n \text{ even} \end{cases}$$

and similarly for G_{sum} . The code for evaluating the functions F_{sum} and G_{sum} is found in Appendix E.

Evaluating $J(1)$ in the case that the boundary of the light source intersects the $z = 0$ plane also requires a boundary integral over D (Equation 17), denoted K , given by

$$K \equiv \int_D (xdy - ydx).$$

D is a unit circle in the xy plane since $z = 0$. We can therefore parameterize D using an angle η via $(\cos \eta, \sin \eta)$. Then,

$$K = \int_{\eta_1}^{\eta_2} [\cos \eta \cos \eta + \sin \eta \sin \eta] d\eta = \int_{\eta_1}^{\eta_2} d\eta = \eta_2 - \eta_1.$$

The angular difference, $\eta_2 - \eta_1$, can be found by determining where C intersects the xy plane. To find the xy projection of the intersections, Q_1 and Q_2 , we substitute the angular endpoints of C , ϕ_1 and ϕ_2 , into Equation 18, as well as the definitions of L , L_1 , and L_2 in terms of ω , to obtain

$$Q_i \equiv \begin{pmatrix} \cos \sigma \sin \omega + \sin \sigma \cos \omega \cos \phi_i \\ \sin \sigma \sin \phi_i \end{pmatrix}$$

for $i = 1, 2$. Then

$$K = \eta_2 - \eta_1 = \cos^{-1}(Q_1 \cdot Q_2).$$

Defining the constants

$$\begin{aligned} c &\equiv \cos \sigma \sin \omega \\ d &\equiv \sin \sigma \cos \omega, \end{aligned}$$

K can be reduced to

$$K = \cos^{-1}((c + d \cos \phi_1)^2 - (\sin \sigma \sin \phi_1)^2). \quad (23)$$

Since the boundary integrals over C were computed from ϕ_1 to ϕ_2 , the integral over D must be computed from ϕ_2 to ϕ_1 . It can be shown that the choice of coordinate system for L , L_1 and L_2 always locates Q_1 in quadrant IV and Q_2 in quadrant I. Thus K from Equation 23 has the correct sense of directionality of the boundary D .

Combining the previous results, we have

$$I(n) = \frac{\sin \sigma}{n+1} [d (F_{\text{sum}}(a, b, n-1, \phi_2) - F_{\text{sum}}(a, b, n-1, \phi_1)) + c (G_{\text{sum}}(a, b, n-1, \phi_2) - G_{\text{sum}}(a, b, n-1, \phi_1))] + \frac{E}{n+1}$$

where

$$E \equiv \begin{cases} I(0), & \text{if } n \text{ is even} \\ K, & \text{if } n \text{ is odd and } -b \leq |a| \\ 0, & \text{otherwise.} \end{cases}$$

Multiplying by the normalization factor of Equation 9, we finally obtain

$$I_{\text{hemi-sub-Phong}}(\omega, \sigma, n) = \begin{cases} 0, & \text{if } \cos \omega \leq -\sin \sigma \\ \frac{1}{2\pi} [\sin \sigma (d\Delta F_{\text{sum}} + c\Delta G_{\text{sum}}) + E], & \text{otherwise} \end{cases} \quad (24)$$

where

$$\begin{aligned} \Delta F_{\text{sum}} &\equiv F_{\text{sum}}(a, b, n-1, \phi_2) - F_{\text{sum}}(a, b, n-1, \phi_1) \\ \Delta G_{\text{sum}} &\equiv G_{\text{sum}}(a, b, n-1, \phi_2) - G_{\text{sum}}(a, b, n-1, \phi_1). \end{aligned}$$

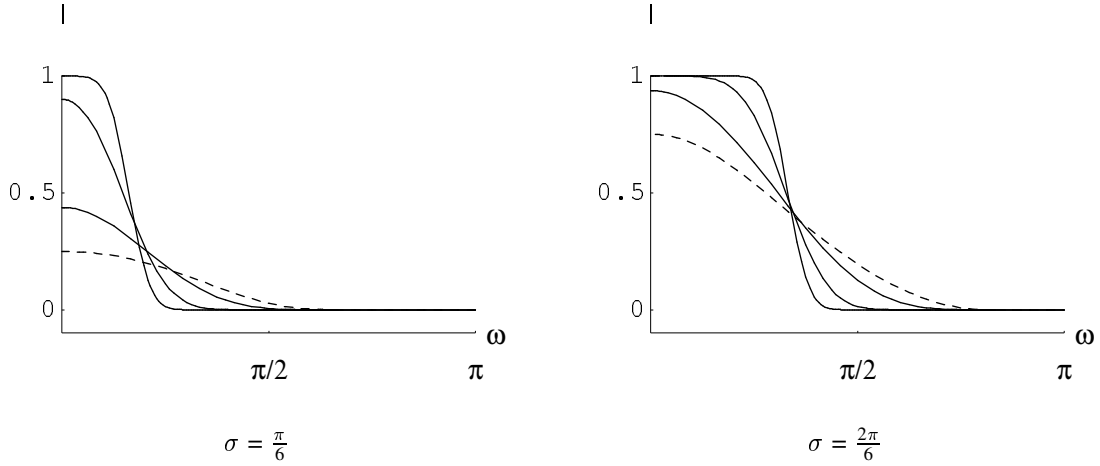


Figure 5: Sub-hemispherical Phong Illumination: The left side plots the sub-hemispherical model for $\sigma = \frac{\pi}{6}$, the right plots for $\sigma = \frac{2\pi}{6}$. Both sides plot intensity versus the angle $\omega \in [0, \pi]$ for values of $n = 1, 3, 15, 63$. The dashed curve represents $n = 1$ on both sides.

Figure 5 compares $I_{\text{hemi-sub-Phong}}$ for various values of σ , ω , and n . Note that $I_{\text{hemi-sub-Phong}}$ is a generalization of both $I_{\text{hemi-sub}}$ and $I_{\text{hemi-const-Phong}}$ via

$$\begin{aligned} I_{\text{hemi-const-Phong}}(\omega, n) &= I_{\text{hemi-sub-Phong}}(\omega, \frac{\pi}{2}, n) \\ I_{\text{hemi-sub}}(\omega, \sigma) &= I_{\text{hemi-sub-Phong}}(\omega, \sigma, 1). \end{aligned}$$

Thus, the left side of Figure 4 can be compared to Figure 5, representing results in which $\sigma = \frac{\pi}{2}$.

The function $I_{\text{hemi-sub-Phong}}$ attains its maximum value at $\omega = 0$, for which

$$I_{\text{hemi-sub-Phong}}(0, \sigma, n) = 1 - \cos^{n+1} \sigma.$$

Figure 6 compares normalized Phong shading for various values of σ , where normalized means dividing by $I_{\text{hemi-sub-Phong}}(0, \sigma, n)$.

It remains to discuss the computation of the solid angle subtended by the light source $I(0)$, in the case that n is even. One technique is to avoid computation of $I(0)$ by restricting specular exponents to odd powers. Another is to compute $I(n)$ for the two odd integers n and $n + 2$ that bracket the desired exponent and interpolate to find an approximate result. In the interests of future work, it can be shown that

$$I(0) = 2 \int_{\frac{\pi}{2}-\sigma}^{\pi-\omega} \sqrt{1 - \frac{\cos^2 \sigma}{\sin^2 \theta}} d\theta.$$

Also, in the case that the light source is fully within the hemisphere around R (i.e., $\omega + \sigma \leq \frac{\pi}{2}$), this simpler result applies:

$$I(0) = 2\pi(1 - \cos \sigma).$$

Actual code for evaluation of the sub-hemispherical Phong model can be found in Appendix F. As in the case of Lambertian lighting, a finite spherical light source can be modeled by computing σ via Equation 7. An infinite light source of fixed angular dimension is modeled using a fixed σ , for which $\cos \sigma$ and $\sin \sigma$ can be pre-computed.

3.3 Phong Illumination from Polygonal Light Sources

As in Section 2.3, a polygonal light source is given consisting of m vertices V_1, V_2, \dots, V_m . Using the spherical parameterization of Section 3.2, Equation 16 still applies. The boundary curve of the light source C now becomes the spherical projection of the light source polygon edges.³ Let U_i be the spherical projection of each of the light source vertices, given by

$$U_i = \frac{V_i - P}{\|V_i - P\|}.$$

³As in Section 2.3, the light source polygon must be clipped; in this case to the hemisphere around R rather than N .

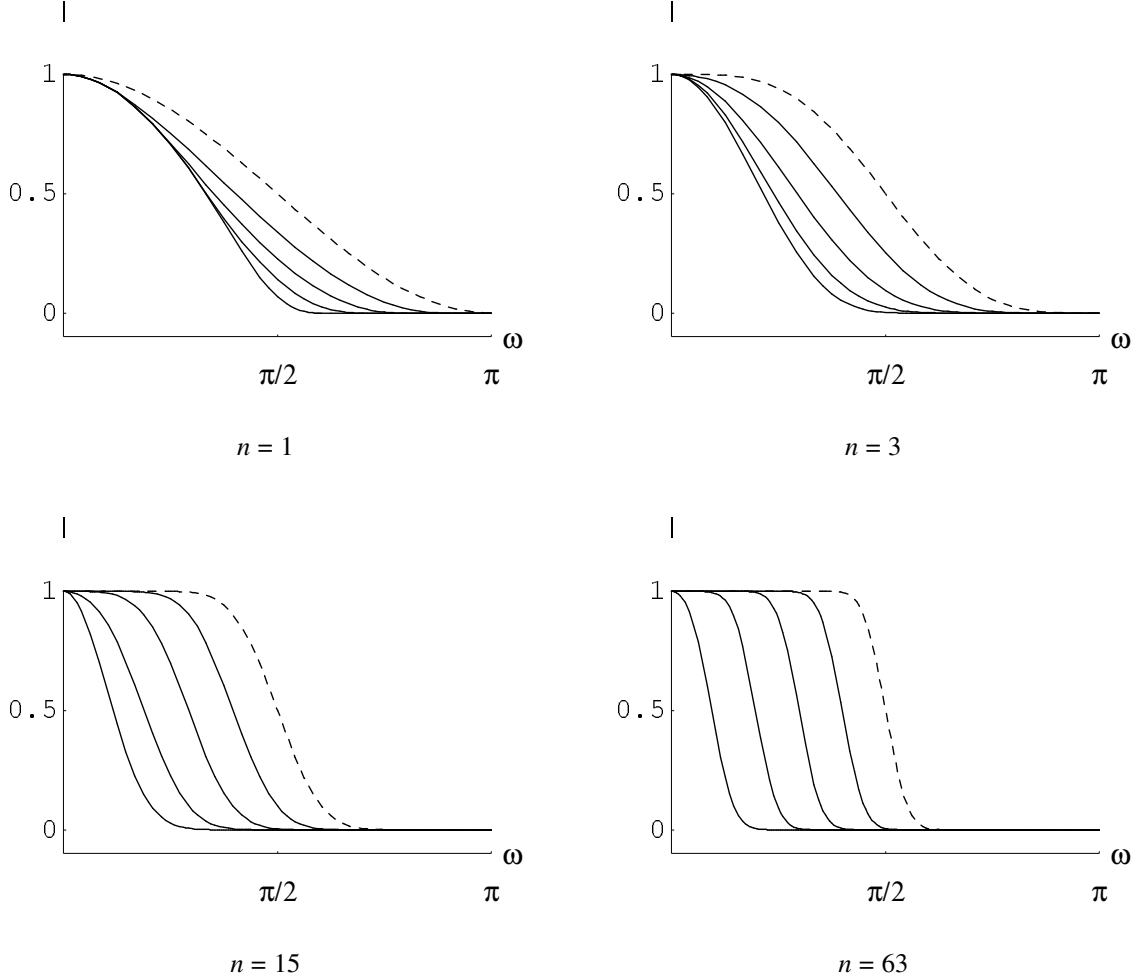


Figure 6: Normalized Sub-hemispherical Phong Illumination: This table compares “normalized” Phong Illumination from sub-hemispherical light sources, where normalized means dividing by the maximum value of the intensity function so as to locate the new maximum value at 1. Each plot fixes the Phong exponent, at $n = 1$, $n = 3$, $n = 15$, and $n = 63$, and displays intensity vs. ω curves for $\sigma = \frac{5}{10}\pi, \frac{4}{10}\pi, \frac{3}{10}\pi, \frac{2}{10}\pi, \frac{1}{10}\pi$. The dashed curve represents $\sigma = \frac{\pi}{2}$ in all plots.

Let Γ_i be the vector perpendicular to U_i and U_{i+1}

$$\Gamma_i \equiv U_i \times U_{i+1}$$

and Γ_i^\perp be the vector perpendicular to U_i and Γ_i :

$$\Gamma_i^\perp \equiv \Gamma_i \times U_i.$$

Then the spherical projection of the edge between V_i and V_{i+1} is given by

$$C_i(\phi) = U_i \cos \phi + \Gamma_i^\perp \sin \phi.$$

where ϕ goes from 0 on U_i to $\cos^{-1}(U_i \cdot U_{i+1})$ on U_{i+1} . Then

$$dC_i = (-U_i \sin \phi + \Gamma_i^\perp \cos \phi) d\phi.$$

On the i -th polygon edge, we finally obtain

$$z_i = R \cdot C_i = R \cdot U_i \cos \phi + R \cdot \Gamma_i^\perp \sin \phi$$

and

$$(xdy - ydx)_i = R \cdot (C_i \times dC_i) = R \cdot \Gamma_i,$$

the analogs of Equations 19 and 20 on this boundary. Note that the factor $(xdy - ydx)_i$ is a constant independent of ϕ . Integrating over C_i in $J(n)$ thus requires integrals of the form

$$T(a_i, b_i, n, x_i) \equiv \int_0^x (a \cos \phi + b \sin \phi)^n d\phi$$

where

$$\begin{aligned} a_i &= R \cdot U_i \\ b_i &= R \cdot \Gamma_i^\perp \\ x_i &= \cos^{-1}(U_i \cdot U_{i+1}). \end{aligned}$$

Using integration by parts, a recurrence relation can be derived for T via

$$T(a, b, n, x) = \frac{1}{n} [(a \cos x + b \sin x)^{n-1} (a \sin x - b \cos x) + a^{n-1} b + (n-1)(a^2 + b^2)T(a, b, n-2, x)]$$

with

$$\begin{aligned} T(a, b, 0, x) &= x \\ T(a, b, 1, x) &= a \sin x - b \cos x + b. \end{aligned}$$

As in Section 3.2, we define the series function T_{sum} via

$$T_{\text{sum}}(a, b, n, x) \equiv \begin{cases} \sum_{i=0}^{\frac{n-1}{2}} T(a, b, 2i+1, x), & \text{if } n \text{ odd} \\ \sum_{i=0}^{\frac{n}{2}} T(a, b, 2i, x), & \text{if } n \text{ even} \end{cases}$$

The code for evaluating the function T_{sum} can be found in Appendix G.

Multiplying by the normalization factor of Equation 9, we finally obtain

$$I_{\text{poly-Phong}} \equiv \frac{1}{2\pi} \begin{cases} \sum_{i=1}^m T_{\text{sum}}(a_i, b_i, n-1, x_i), & \text{if } n \text{ odd} \\ I(0) + \sum_{i=1}^m T_{\text{sum}}(a_i, b_i, n-1, x_i), & \text{if } n \text{ even} \end{cases} \quad (25)$$

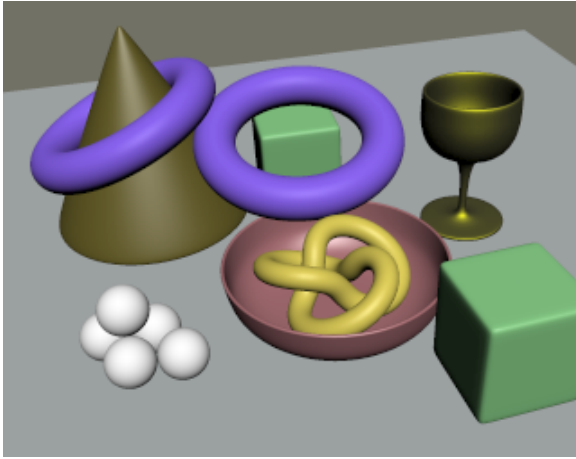
As before, we can avoid evaluation of the solid angle subtended by the light source $I(0)$ by restricting Phong exponents to odd integers. See [Arvo95] for details on computing solid angles for polygonal sources. Code for evaluating $I_{\text{poly-Phong}}$ is given in Appendix H. The same code suffices for computing the Lambertian lighting of Section 2.3. Note that the code performs clipping of the light source polygon with respect to the hemisphere around R (or N) as it sums edge contributions.

4 Summary

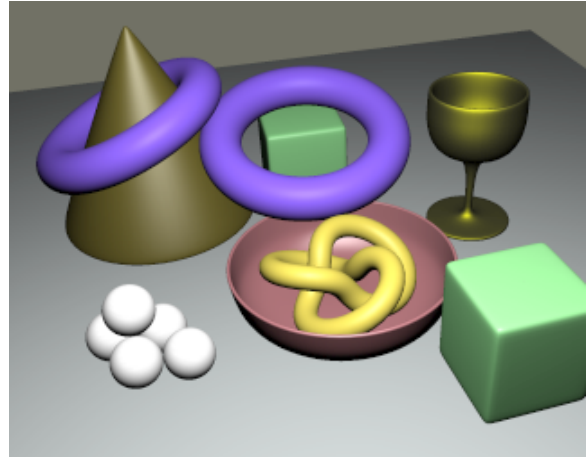
The following table summarizes the results in this paper.

Lighting Model	Light Source	Name	Equation Number
Lambertian	constant-weighted hemisphere	$I_{\text{hemi-const}}$	(3)
Lambertian	cosine-weighted hemisphere	$I_{\text{hemi-cos}}$	(5)
Lambertian	constant-weighted sub-hemisphere	$I_{\text{hemi-sub}}$	(6)
Lambertian	constant-weighted polygon	I_{poly}	(8)
Phong	constant-weighted hemisphere	$I_{\text{hemi-const-Phong}}$	(14)
Phong	cosine-weighted hemisphere	$I_{\text{hemi-cos-Phong}}$	(15)
Phong	constant-weighted sub-hemisphere	$I_{\text{hemi-sub-Phong}}$	(24)
Phong	constant-weighted polygon	$I_{\text{poly-Phong}}$	(25)

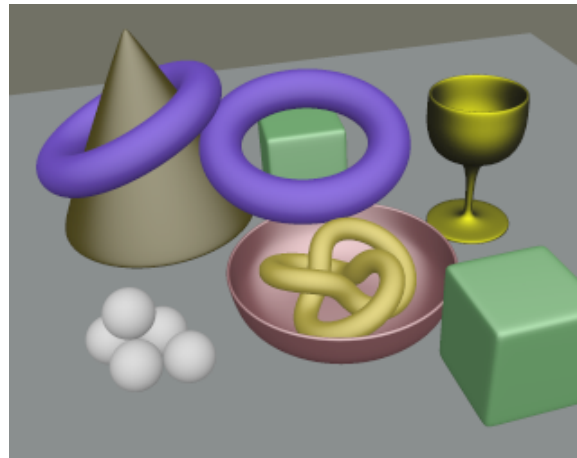
Figure 7 compares images using some of the area light source models with traditional point light source models.



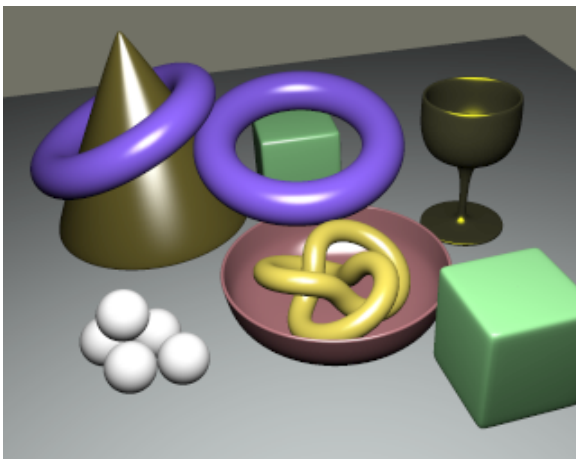
(a) Non-Area Directional



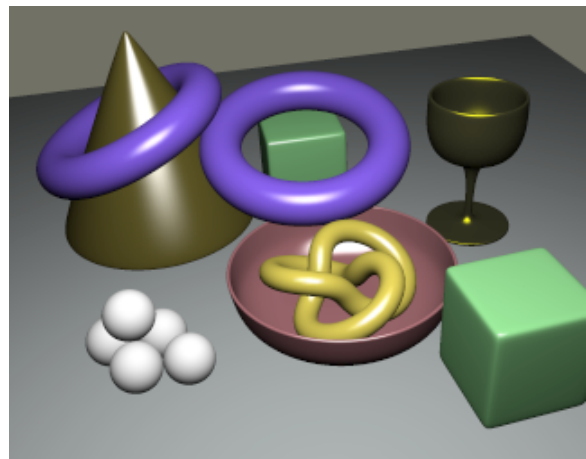
(b) Non-Area Positional



(c) Overcast Sky Hemispherical Light Source



(d) Finite Spherical



(e) Polygonal

Figure 7: Comparison of Area Light Source Results.

References

- [Arvo94] Arvo, James, “The Irradiance Jacobian for Partially Occluded Polyhedral Sources,” Siggraph 94, July 1994, 343-350.
- [Arvo95] Arvo, James, “Applications of Irradiance Tensors to the Simulation of Non-Lambertian Phenomena,” Siggraph 95, August 1995, 335-342.
- [Nishita85] Nishita, Tomoyuki, and Eihachiro Nakamae, “Continuous Tone Representation of Three-Dimensional Taking Account of Shadows and Interreflection,” Siggraph 85, July 1985, 23-30.
- [Nishita86] Nishita, Tomoyuki, and Eihachiro Nakamae, “Continuous Tone Representation of Three-Dimensional Objects Illuminated by Sky Light,” Siggraph 86, August 1986, 125-132.

A Derivation of Lambertian Luminance from Sub-Hemispherical Light Sources

This section derives Equation 6. The region of integration has three distinct forms: first, in which the sub-hemispherical light source is entirely within the hemisphere around the normal, second, in which the light source is partially within the normal’s hemisphere, and finally, in which the light source is entirely outside the normal’s hemisphere. These cases may be detected using the following test on ω , the angle between L and N :

$$\begin{aligned} \omega \in [0, \frac{\pi}{2} - \sigma] &\rightarrow \text{entirely inside} \\ \omega \in [\frac{\pi}{2} - \sigma, \frac{\pi}{2} + \sigma] &\rightarrow \text{partially inside} \\ \omega \in [\frac{\pi}{2} + \sigma, \pi] &\rightarrow \text{entirely outside} \end{aligned}$$

Clearly, the value of the integral will be zero in the last case.

In the case that the light source is entirely within the normal’s hemisphere, we perform the integration analytically by parameterizing the subsphere about L via

$$p(\theta, \phi) \equiv \begin{pmatrix} \cos \theta \sin \phi \\ \sin \theta \sin \phi \\ \cos \phi \end{pmatrix}$$

where $\theta \in [0, 2\pi]$ and $\phi \in [0, \sigma]$. The coordinate system is transformed so that L maps to the z -axis. The normal represented in this coordinate system is

$$N = \begin{pmatrix} \sin \omega \\ 0 \\ \cos \omega \end{pmatrix}.$$

Note that this is different than the parameterization used in Section 2.1 in that we parameterize around the light source direction rather than the normal. The unnormalized integral from Equation 1 then reduces to

$$I = \int_0^{2\pi} d\theta \int_0^\sigma d\phi [\sin \omega \cos \theta \sin \phi + \cos \omega \cos \phi] \sin \phi$$

since

$$dA = \sin \phi d\phi d\theta$$

and

$$p \cdot N = \cos \theta \sin \phi \sin \omega + \cos \phi \cos \omega.$$

This integral is easily evaluated to yield

$$I = \pi \cos \omega \sin^2 \sigma$$

which forms the first case in Equation 2.

The second case is more difficult. We transform coordinates and parameterize the light source region via

$$p(\theta, \phi) \equiv \begin{pmatrix} \cos \theta \sin \phi \\ -\cos \phi \\ \sin \theta \sin \phi \end{pmatrix}$$

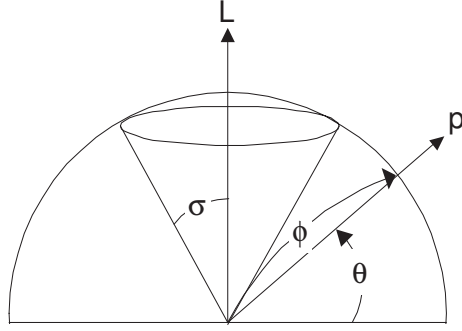


Figure 8: Subhemispherical parameterization: The light source region is the part of the hemisphere around L that makes an angle of no more than σ with L . θ parameterizes the angle between L and the perpendicular projection of N onto L ; ϕ , the angle in the plane perpendicular to L and N .

with

$$N = \begin{pmatrix} \sin \omega \\ 0 \\ \cos \omega \end{pmatrix}.$$

Here L has been transformed to map onto the z -axis, and the plane formed by N and L becomes the xz plane (Figure 8). The parameter domain is a subset of $\theta, \phi \in [0, \pi]$, representing the full hemisphere around L , intersected with the angular extent of the light source and the hemisphere around N . We denote the appropriate integral domain as H' . We thus have

$$I = \int \int_{H'} [\sin \omega \cos \theta + \cos \omega \sin \theta] \sin^2 \phi \, d\theta \, d\phi. \quad (26)$$

Using Gauss' integral theorem, which states

$$\int \int_D (\partial Q / \partial x - \partial P / \partial y) \, dD = \int_C P \, dx + Q \, dy,$$

we can transform the above iterated integral into a 1D integral around the boundary of the region H' , denoted C . Let

$$\begin{aligned} Q &= \sin^2 \phi [\sin \omega \sin \theta - \cos \omega \cos \theta] \\ P &= 0 \end{aligned}$$

in Gauss' theorem. Then $\partial Q / \partial \theta - \partial P / \partial \phi$ is equal to the integrand in Equation 26. So Equation 26 reduces to

$$\int_C \sin^2 \phi [\sin \omega \sin \theta - \cos \omega \cos \theta] \, d\phi \quad (27)$$

The boundary curves are of two types. One type forms the circular boundary of the light source. On this boundary,

$$p(\theta, \phi) \cdot \begin{pmatrix} 0 \\ 0 \\ 1 \end{pmatrix} = \cos \sigma \Rightarrow \sin \theta \sin \phi = \cos \sigma \quad (28)$$

since the incident light direction makes an angle of exactly σ with L , which maps to the z -axis in the transformed coordinate system. Thus, on this boundary, we have

$$\begin{aligned} \sin \theta &= \frac{\cos \sigma}{\sin \phi} \\ \cos \theta &= \begin{cases} +\sqrt{1 - \frac{\cos^2 \sigma}{\sin^2 \phi}}, & \theta \leq \frac{\pi}{2} \\ -\sqrt{1 - \frac{\cos^2 \sigma}{\sin^2 \phi}}, & \theta > \frac{\pi}{2} \end{cases} \end{aligned}$$

The second boundary is an constant- θ boundary formed where the normal's hemisphere intersects the light source. Note that the parameterization (with θ parameterizing the angle in the plane formed by L and N) is explicitly chosen so that this intersection forms such a simple curve. The normal hemisphere intersection with the hemisphere around L occurs where $\theta = \pi - \omega$.

Because of the change in sign in $\cos \theta$, the integration region must be further broken down. The boundary of the light source must be separated into segments where $\theta \leq \frac{\pi}{2}$ and $\theta > \frac{\pi}{2}$. In one case (Figures 9), the normal hemisphere intersects the light source at $\theta \geq \frac{\pi}{2}$. This happens when $\omega \in [\frac{\pi}{2} - \sigma, \frac{\pi}{2}]$. The boundary of the integration region consists of five segments. For larger ω (Figure 10), the normal hemisphere intersects the light source at $\theta < \frac{\pi}{2}$. The boundary of the integration region consists of three segments.

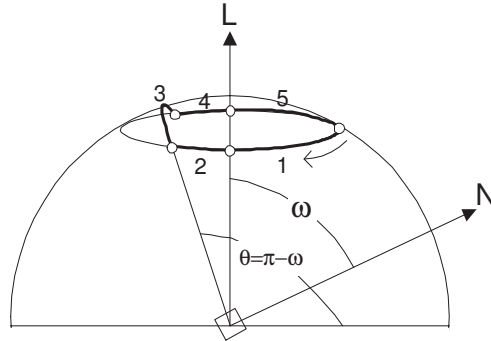


Figure 9: Boundary curves for $\omega \in [\frac{\pi}{2} - \sigma, \frac{\pi}{2}]$: In this case the normal's hemisphere intersects the light source at $\pi - \omega \geq \frac{\pi}{2}$.

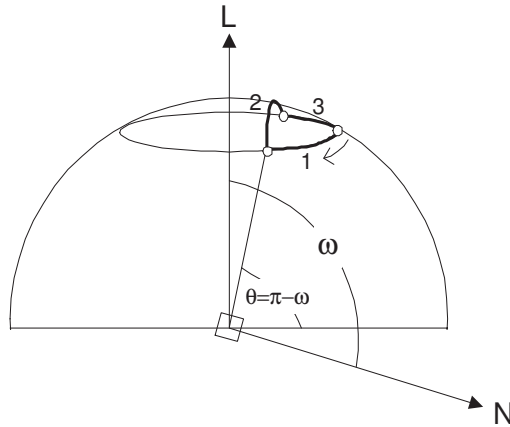


Figure 10: Boundary curves for $\omega \in [\frac{\pi}{2}, \frac{\pi}{2} + \sigma]$: Here, the normal's hemisphere intersects the light source at $\pi - \omega \leq \frac{\pi}{2}$.

On a circular boundary segment (segments 1, 2, 4, and 5 from Figure 9, segments 1 and 3 from Figure 10), the boundary integral in Equation 27 reduces to

$$I_{\text{circle}}(\phi_1, \phi_2, \theta\text{-quadrant}) \equiv \int_{\phi_1}^{\phi_2} \sin^2 \phi \left[\sin \omega \frac{\cos \sigma}{\sin \phi} \mp \cos \omega \sqrt{1 - \frac{\cos^2 \sigma}{\sin^2 \phi}} \right] d\phi$$

where the top (−) of the \mp is used when $\theta\text{-quadrant} = 1$ (i.e., $\theta \leq \frac{\pi}{2}$) and the bottom (+) of the \mp is used when $\theta\text{-quadrant} = 2$

(i.e., $\theta > \frac{\pi}{2}$). The integral reduces to

$$-\sin \omega \cos \sigma \left[\cos \phi \right] \Big|_{\phi_1}^{\phi_2} \mp \cos \omega \int_{\phi_1}^{\phi_2} \sin \phi \sqrt{\sin^2 \sigma - \cos^2 \phi} d\phi.$$

But the following relation holds

$$\int \sqrt{a^2 - \cos^2 x} \sin x dx = -\frac{1}{2} \left[\cos x \sqrt{a^2 - \cos^2 x} + a^2 \sin^{-1} \left(\frac{\cos x}{a} \right) \right].$$

Therefore, we have

$$I_{\text{circle}} = -\sin \omega \cos \sigma \left[\cos \phi \right] \Big|_{\phi_1}^{\phi_2} \mp \frac{1}{2} \cos \omega \left[\cos \phi \sqrt{\sin^2 \sigma - \cos^2 \phi} + \sin^2 \sigma \sin^{-1} \left(\frac{\cos \phi}{\sin \sigma} \right) \right] \Big|_{\phi_1}^{\phi_2}. \quad (29)$$

On a constant- θ boundary segment (segment 3 from Figure 9 or segment 2 from Figure 10), the boundary integral in Equation 27 reduces to

$$I_{\text{iso-}\theta}(\phi_1, \phi_2, \theta) \equiv \frac{1}{2} [\sin \omega \sin \theta - \cos \omega \cos \theta] \left[\phi - \sin \phi \cos \phi \right] \Big|_{\phi_1}^{\phi_2} \quad (30)$$

Using these definitions, we can now perform the boundary integrals. We start with the situation illustrated in Figure 9, where $\omega \in [\frac{\pi}{2} - \sigma, \frac{\pi}{2}]$. Note that for any value of θ , the corresponding value of ϕ on the circular boundary curve (segments 1, 2, 4, and 5) takes on two values (refer to Equation 28), given by

$$\phi^1(\theta) \equiv \sin^{-1} \left(\frac{\cos \sigma}{\sin \phi} \right)$$

and

$$\phi^2(\theta) \equiv \pi - \sin^{-1} \left(\frac{\cos \sigma}{\sin \phi} \right)$$

where ϕ^1 is an angle in quadrant 1 ($\leq \frac{\pi}{2}$) and ϕ^2 is in quadrant 2, ($> \frac{\pi}{2}$).⁴ We obtain the following table of (θ, ϕ) pairs at the endpoints of the circular boundary segments:

$$\begin{array}{c|ccc} \theta & \frac{\pi}{2} - \sigma & \frac{\pi}{2} & \pi - \omega \\ \phi^1 & \frac{\pi}{2} & \frac{\pi}{2} - \sigma & \gamma \\ \phi^2 & \frac{\pi}{2} & \frac{\pi}{2} + \sigma & \pi - \gamma \end{array}$$

where

$$\gamma \equiv \sin^{-1} \left(\frac{\cos \sigma}{\sin(\pi - \omega)} \right) = \sin^{-1} \left(\frac{\cos \sigma}{\sin \omega} \right).$$

Summing the curve integrals over the boundary segments, we obtain

$$I = I_{\text{circle}}\left(\frac{\pi}{2}, \frac{\pi}{2} - \sigma, 1\right) + I_{\text{circle}}\left(\frac{\pi}{2} - \sigma, \gamma, 2\right) + I_{\text{iso-}\theta}(\gamma, \pi - \gamma, \pi - \omega) + I_{\text{circle}}\left(\pi - \gamma, \frac{\pi}{2} + \sigma, 2\right) + I_{\text{circle}}\left(\frac{\pi}{2} + \sigma, \frac{\pi}{2}, 1\right)$$

where the terms are derived from the segments in the order 1, 2, 3, 4, and 5. Substituting Equations 29 and 30 yields

$$\begin{aligned} I &= -\sin \omega \cos \sigma \left[\cos \phi \right] \left(\left| \frac{\pi}{2} \right|_{\frac{\pi}{2}-\sigma} + \left| \frac{\pi}{2}-\sigma \right|_{\gamma} + \left| \pi-\gamma \right|_{\frac{\pi}{2}+\sigma} + \left| \frac{\pi}{2}+\sigma \right|_{\frac{\pi}{2}} \right) + \\ &\quad \frac{1}{2} \cos \omega \left[\cos \phi \sqrt{\sin^2 \sigma - \cos^2 \phi} + \sin^2 \sigma \sin^{-1} \left(\frac{\cos \phi}{\sin \sigma} \right) \right] \left(\left| \frac{\pi}{2} \right|_{\frac{\pi}{2}-\sigma} + \left| \gamma \right|_{\frac{\pi}{2}-\sigma} + \left| \frac{\pi}{2}+\sigma \right|_{\pi-\gamma} + \left| \frac{\pi}{2}+\sigma \right|_{\frac{\pi}{2}} \right) + \\ &\quad \frac{1}{2} [\sin \omega \sin \theta - \cos \omega \cos \theta] \left[\phi - \sin \phi \cos \phi \right] \Big|_{\pi-\gamma}^{\gamma}. \end{aligned}$$

⁴This assumes \sin^{-1} refers to the principal value of the inverse sine, returning an argument in the range $[-\frac{\pi}{2}, \frac{\pi}{2}]$. Since $\sigma \in [0, \frac{\pi}{2}]$ and $\phi \in [0, \pi]$, the ratio of the argument of \sin^{-1} in the definition of ϕ^1 is therefore positive, so an angle in the range $[0, \frac{\pi}{2}]$ is returned.

Since

$$\sin \omega \sin(\pi - \omega) - \cos \omega \cos(\pi - \omega) = 1,$$

this reduces finally to

$$I = \pi \cos \omega \sin^2 \sigma - \cos \omega \left[\cos \gamma \sqrt{\sin^2 \sigma - \cos^2 \gamma} + \sin^2 \sigma \sin^{-1} \left(\frac{\cos \gamma}{\sin \sigma} \right) \right] - 2 \sin \omega \cos \sigma \cos \gamma + \frac{\pi}{2} - \gamma + \sin \gamma \cos \gamma,$$

as in Equation 6.

The derivation for the situation illustrated in Figure 10 is similar. Integrating over the three boundary segments, we obtain

$$I = I_{\text{circle}}\left(\frac{\pi}{2}, \gamma, 1\right) + I_{\text{iso-}\theta}(\gamma, \pi - \gamma, \pi - \omega) + I_{\text{circle}}\left(\pi - \gamma, \frac{\pi}{2}, 1\right)$$

which yields

$$\cos \omega \left[\cos \gamma \sqrt{\sin^2 \sigma - \cos^2 \gamma} + \sin^2 \sigma \sin^{-1} \left(\frac{\cos \gamma}{\sin \sigma} \right) \right] - 2 \sin \omega \cos \sigma \cos \gamma + \frac{\pi}{2} - \gamma + \sin \gamma \cos \gamma,$$

as in Equation 6.

B Code for Sine Power Integral Evaluation

```

/*
-----
sine_power_integral

Recurrence algorithm for computing the parameterized function

    S(n,x) = integral(sin(x)^n dx)

where S(n,0) = 0 (i.e., integral is from 0 to x).

The function for the first few integers has the following form:

    S(0,x) = x
    S(1,x) = 1-cos(x)
    S(2,x) = x/2 - 1/4 sin(2 x)
    .
    .
    .

The appropriate recurrence relation here is

    S(n,x) = 1/n ( -sin(x)^(n-1) cos(x) + (n-1) S(n-2,x) )

Note: the argument x is unused if n is odd.
-----
*/
double sine_power_integral(int n,double x,double cos_x,double sin_x)
{
    double S,G;
    int i,start;
    double sin_x_sq = sin_x*sin_x;

    /* initial conditions for recurrence */
    if (n&1) { /* n is odd */
        /* Note: parameter x unused! */
        S = 1-cos_x;
        G = sin_x_sq*cos_x;
        start = 1;
    } else { /* n is even */
        S = x;
        G = sin_x*cos_x;
        start = 0;
    }
}

```

```

/* iterate recurrence upward */
for (i = start+2; i <= n; i += 2) {

    /* compute S(i) from S(i-2) */
    S = ((i-1)*S - G)/i;
    G *= sin_x_sq;
}

return S;
}

```

C Stokes' Theorem Derivation of Boundary Integral Series for Specular Integral

Stokes' Theorem states that

$$\int_{\Omega} N \cdot (\nabla \times V) d\Omega = \oint_{\partial\Omega} V \cdot dr$$

where N is the normal to the surface Ω , V is a vector function over this surface, $\partial\Omega$ is the closed curve forming the boundary of Ω , and $r = (x, y, z)$ are the surface parameters. Letting

$$V \equiv \begin{pmatrix} -\frac{1}{2}yz^{n-1} \\ \frac{1}{2}xz^{n-1} \\ 0 \end{pmatrix},$$

and noting that

$$N = \begin{pmatrix} x \\ y \\ z \end{pmatrix}$$

for a sphere, we have

$$\int_{\Omega} (\nabla \times V) \cdot \begin{pmatrix} x \\ y \\ z \end{pmatrix} = \frac{1}{2} \oint_{\partial\Omega} z^{n-1} (xdy - ydx) \quad (31)$$

by Stokes' Theorem. Expanding $(\nabla \times V) \cdot N$, we have

$$\begin{aligned} (\nabla \times V) \cdot N &= -\frac{1}{2}(n-1)x^2z^{n-2} + -\frac{1}{2}y^2z^{n-2} + z^n \\ &= z^n - \frac{1}{2}(n-1)(1-z^2)z^{n-2} \end{aligned} \quad (32)$$

since $x^2 + y^2 = 1 - z^2$ on the sphere.

We define $I(n)$ as the surface integral

$$I(n) \equiv \int_{\Omega} z^n d\Omega$$

and $J(n)$ as the boundary integral

$$J(n) \equiv \oint_{\partial\Omega} z^{n-1} (xdy - ydx).$$

Substituting the result from Equation 32 in Equation 31, and using the above definitions, yields

$$I(n) - \frac{1}{2}(n-1)[I(n-2) - I(n)] = \frac{1}{2}J(n).$$

Rearranging, we have

$$I(n) = \frac{n-1}{n+1}I(n-2) + \frac{1}{n+1}J(n) \quad (33)$$

Two observations can be used to define the termination criteria for the above recurrence. First, from the definition of $I(n)$, $I(0)$ can be seen to represent the solid angle subtended by Ω . Second, substituting $n = 1$, we have

$$I(1) = \frac{1}{2}J(1).$$

From the recurrence relation and these termination criteria, it can easily be proved by induction that

$$I(n) = \begin{cases} \frac{1}{n+1} \sum_{i=0}^{\frac{n-1}{2}} J(2i+1), & \text{for } n \text{ odd} \\ \frac{1}{n+1} \left[I(0) + \sum_{i=1}^{\frac{n}{2}} J(2i) \right], & \text{for } n \text{ even.} \end{cases}$$

Note that the above definition uses $J(n)$ for $n > 0$ (i.e., $J(0)$ is not required).

D Recurrence Relations for Integrals of the form $(a + b \cos \phi)^n$

This section derives a recurrence relation for calculating integrals of the form

$$F(a, b, n, x) \equiv \int_0^x (a + b \cos \phi)^n d\phi$$

and

$$G(a, b, n, x) \equiv \int_0^x (a + b \cos \phi)^n \cos \phi d\phi.$$

We first define an auxiliary function H via

$$H(a, b, n, x) \equiv \int_0^x (a + b \cos \phi)^n \cos^2 \phi d\phi.$$

Then,

$$\begin{aligned} F(a, b, n, x) &= \int_0^x (a + b \cos \phi)^n d\phi \\ &= \int_0^x (a + b \cos \phi)(a + b \cos \phi)^{n-1} d\phi \\ &= aF(a, b, n-1, x) + bG(a, b, n-1, x). \end{aligned}$$

Also,

$$\begin{aligned} G(a, b, n, x) &= \int_0^x (a + b \cos \phi)^n \cos \phi d\phi \\ &= \int_0^x (a + b \cos \phi)(a + b \cos \phi)^{n-1} \cos \phi d\phi \\ &= aG(a, b, n-1, x) + bH(a, b, n-1, x). \end{aligned}$$

This implies

$$H(a, b, n-1, x) = \frac{1}{b} (G(a, b, n, x) - aG(a, b, n-1, x)). \quad (34)$$

Using integration by parts, we also have

$$\begin{aligned} G(a, b, n, x) &= \int_0^x (a + b \cos \phi)^n \cos \phi d\phi \\ &= \left[(a + b \cos \phi)^n \sin \phi \right] \Big|_0^x + nb \int_0^x \sin^2 \phi (a + b \cos \phi)^{n-1} d\phi \\ &= (a + b \cos x)^n \sin x + nb [F(a, b, n-1, x) - H(a, b, n-1, x)]. \end{aligned}$$

Substituting Equation 34 into the above,

$$G(a, b, n, x) = (a + b \cos x)^n \sin x + nb \left[F(a, b, n - 1, x) - \frac{G(a, b, n, x) - aG(a, b, n - 1, x)}{b} \right].$$

The final recurrence is given by

$$F(a, b, n, x) = aF(a, b, n - 1, x) + bG(a, b, n - 1, x) \quad (35)$$

$$G(a, b, n, x) = \frac{1}{n+1} [(a + b \cos x)^n \sin x + n (bF(a, b, n - 1, x) + aG(a, b, n - 1, x))]. \quad (36)$$

The termination criteria are given by

$$F(a, b, 0, x) = x \quad (37)$$

$$G(a, b, 0, x) = \sin x. \quad (38)$$

Note that the $(a + b \cos x) \sin x$ term in the above recurrence is 0, and can therefore be eliminated, when this integral is applied to the Phong illumination from sub-hemispherical light source problem (Eqns. 21 and 22). The code in Appendix E reflects this optimization.

E Code for Evaluation of Finite Series of Integrals of Form $(a + b \cos \phi)^n$

```

/*
-----
cosine_const_power_integral_sum

Computes the sum

    Fsum(theta,n,a,b) = Sum_{i=0}^{n/2} F(theta,2i,a,b), if n is even
                      Sum_{i=0}^{(n-1)/2} F(theta,2i+1,a,b), if n is odd

where the function F is defined as

    F(theta,n,a,b) = integral( [a + b cos(theta)]^n d theta )
and where F(0,n,a,b) = 0 (i.e., integral is from 0 to theta).

As a by-product, also computes the functions

    G(theta,n,a,b) = integral( [a + b cos(theta)]^n cos(theta) d theta )

The recurrence relation for F is

    F(theta,n,a,b) = a F(theta,n-1,a,b) + b G(theta,n-1,a,b,c)

    G(theta,n,a,b) = n/(n+1) [ b F(n-1) + a G(n-1) ]

The routine assumes that either sin(theta) = 0, or a + b cos(theta) = 0,
allowing a simplification in the general recurrence relation.

Returns the sums of F and G as last two arguments.
-----
*/

#define EVEN(i)  (((i)&1) == 0)

void cosine_const_power_integral_sum(double theta,double sin_theta,
                                     int n,double a,double b,
                                     double *_Fsum,double *_Gsum)
{
    double F,G,Fsum,Gsum;
    int i;

```

```

/* initial conditions for recurrence */
F = theta;
G = sin_theta;
if (EVEN(n)) {
    Fsum = F;
    Gsum = G;
} else {
    Fsum = Gsum = 0;
}

/* iterate recurrence upward */
for (i = 1; i <= n; i++) {

    /* compute F(i),G(i) from F(i-1),G(i-1) */
    double Fnew = a*F + b*G;
    double Gnew = (i*(b*F + a*G))/(i+1);

    F = Fnew;
    G = Gnew;

    /* accumulate sums of F and G */
    if (EVEN(n+i)) {
        Fsum += F;
        Gsum += G;
    }
}

*_Fsum = Fsum;
*_Gsum = Gsum;
}

```

F Code for Evaluation of Sub-hemispherical Phong Illumination

```

/*
shd_subsphere_specular

Computes integral over subsphere of specular lighting.

Parameters:
-----

cos_omega, sin_omega: cosine and sine of omega, the angle between the the light source central
axis and the reflection direction

cos_sigma, sin_sigma: cosine and sine of sigma, the angular size of the light source.
Sigma must be <= Pi/2; i.e., cos_sigma, sin_sigma >= 0.

e:          specular exponent (currently converted to odd integer to speed things up)

Returns the specular reflectance result.
*/
double shd_subsphere_specular(double cos_omega,double sin_omega,double cos_sigma,double sin_sigma,int e)
{
    double a = cos_sigma*cos_omega;
    double b = -sin_sigma*sin_omega;
    double c = cos_sigma*sin_omega;
    double d = sin_sigma*cos_omega;
    double phi1,cos_phi1,sin_phi1;
    double phi2,sin_phi2;
    double Fsum1,Gsum1,Fsum2,Gsum2;
    double E;

    /* light source must be in hemisphere around reflection direction (omega >= Pi/2 + sigma) */
    if (cos_omega <= -sin_sigma) return 0;

```

```

/* make exponent odd */
if ((e & 1) == 0) e = e+1;

/* find integration limits */
if (fabs(a) > -b) {

    /* light source boundary wholly within hemisphere */
    phil = 0;
    phi2 = 2*M_PI;
    cos_phil = 1;
    sin_phil = sin_phi2 = 0;
    E = 0;

} else {

    /* light source boundary partially outside hemisphere */
    /*
     * b is always negative, so take decreasing cosine
     * so that a+b cos(phi) is positive for phi between
     * phil and phi2.
     */

    cos_phil = -a/b;
    sin_phil = sqrt(1 - cos_phil*cos_phil);
    phil = acos(cos_phil);
    sin_phi2 = -sin_phil;
    phi2 = 2*M_PI - phil;

    { /* compute contribution from boundary/hemisphere intersection */
        double x = c+d*cos_phil;
        double y1 = sin_sigma*sin_phil;
        double y2 = sin_sigma*sin_phi2;
        E = acos(x*x + y1*y2);
    }

}

cosine_const_power_integral_sum(phil,sin_phil,e-1,a,b,&Fsum1,&Gsum1);
cosine_const_power_integral_sum(phi2,sin_phi2,e-1,a,b,&Fsum2,&Gsum2);
return (sin_sigma*(d*(Fsum2-Fsum1) + c*(Gsum2-Gsum1)) + E)/(2*M_PI);
}

```

G Code for Evaluation of Finite Series of Integrals of Form $(a \cos \theta + b \sin \theta)^n$

```

/*
-----
cosine_sine_power_integral_sum

Computes the sum

    Tsum(theta,n,a,b) = Sum_{i=0}^{n/2} T(theta,2i,a,b), if n is even
                      Sum_{i=0}^{(n-1)/2} T(theta,2i+1,a,b), if n is odd

where the function T is defined as

    T(theta,n,a,b) = integral( [a cos(theta) + b sin(theta)]^n d theta )

and where T(0,n,a,b) = 0 (i.e., integral is from 0 to theta).

The recurrence relation is

    T(theta,n,a,b) = 1/n [ (a sin(theta) - b cos(theta)) (a cos(theta) + b sin(theta))^(n-1) +
                          a^(n-1) b + (n-1) (a^2 + b^2) T(theta,n-2,a,b) ]

-----
*/

```

```

double cosine_sine_power_integral_sum(double theta,double cos_theta,double sin_theta,
                                     int n,double a,double b)
{
    double f = a*a + b*b;
    double g = a*cos_theta + b*sin_theta;
    double gsq = g*g;
    double asq = a*a;
    double h = a*sin_theta - b*cos_theta;
    double T,Tsum;
    double l,l2;
    int i,start;

    /* initial conditions for recurrence */
    if (n&1) { /* n is odd */
        T = h+b;
        l = gsq*h;
        l2 = b*asq;
        start = 1;
    } else { /* n is even */
        T = theta;
        l = g*h;
        l2 = b*a;
        start = 0;
    }
    Tsum = T;

    /* iterate recurrence upward */
    for (i = start+2; i <= n; i += 2) {

        /* compute T(i) from T(i-2) */
        T = (l + l2 + f*(i-1)*T)/i;
        l *= gsq;
        l2 *= asq;
        Tsum += T;
    }

    return Tsum;
}

```

H Code for Evaluation of Polygonal Phong Illumination

```

static void cross(double a[3],double b[3],double c[3])
{
    c[0] = a[1]*b[2] - a[2]*b[1];
    c[1] = a[2]*b[0] - a[0]*b[2];
    c[2] = a[0]*b[1] - a[1]*b[0];
}

static double dot(double a[3],double b[3])
{
    return a[0]*b[0] + a[1]*b[1] + a[2]*b[2];
}

static double length(double v[3])
{
    return sqrt(dot(v,v));
}

static double normalize(double v[3])
{
    double l = length(v);
    if (l > 0) {
        v[0] /= l;
        v[1] /= l;
        v[2] /= l;
    }
}

```

```

    return l;
}

static void diff_vector(double p1[3],double p2[3],double v[3])
{
    v[0] = p1[0] - p2[0];
    v[1] = p1[1] - p2[1];
    v[2] = p1[2] - p2[2];
}

/*
Finds point on line segment where the segment intersects a plane through the origin.
The plane is specified by a normal n. The line
segment is specified by two points: v0 and v1. The point of intersection
is returned in q. The segment is assumed to intersect the plane.
*/
static void seg_plane_intersection(double v0[3],double v1[3],double n[3],double q[3])
{
    double vd[3];
    double t;

    vd[0] = v1[0] - v0[0];
    vd[1] = v1[1] - v0[1];
    vd[2] = v1[2] - v0[2];

    t = -dot(v0,n)/dot(vd,n);

    q[0] = v0[0] + t*vd[0];
    q[1] = v0[1] + t*vd[1];
    q[2] = v0[2] + t*vd[2];
}

#define COPY3(dst,src) (memcpy(dst,src,sizeof(double)*3))

/*
Computes the contribution from a single edge.
*/
static double shd_edge_contribution(double v0[3],double v1[3],double n[3],int e)
{
    double f;
    double cos_theta,sin_theta;
    double q[3];

    cross(v0,v1,q);
    sin_theta = normalize(q);
    cos_theta = dot(v0,v1);

    if (e == 1) {
        f = acos(cos_theta);
    } else {
        double w[3];
        double theta;

        theta = acos(cos_theta);

        cross(q,v0,w);
        f = cosine_sine_power_integral_sum(theta,cos_theta,sin_theta,e-1,dot(v0,n),dot(w,n));
    }

    return f*dot(q,n);
}

/*
Computes the surface integral over the solid angle subtended by a polygon as seen
from the point p in the direction n of

    max(0,dot(n,l))^e dl

```

where l is the projection of the light polygon into the hemisphere surrounding p with zenith direction n , and e is an exponent (1 for diffuse shading, > 1 for specular).

```

nv -- number of vertices in light source
v  -- array of light source vertices
p  -- point to be illuminated
n  -- direction of hemisphere zenith (unit vector)
e  -- exponent
*/
static double shd_polygonal(int nv,double v[][3],double p[3],double n[3],int e)
{
    int i,j,i1;
    double sum = 0;
    double ui0[3],ui1[3]; /* unnormalized vertices of edge */
    double vi0[3],vi1[3]; /* unit-length vector vertices of edge */
    int belowi0,belowi1; /* flag for whether last vertex was below point's "horizon" */

    /* find first vertex above horizon */
    for (j = 0; j < nv; j++) {
        double u[3];
        diff_vector(v[j],p,u);
        if (dot(u,n) >= 0) {
            COPY3(ui0,u);
            COPY3(vi0,u);
            normalize(vi0);
            belowi0 = 0;
            break;
        }
    }
    if (j >= nv) return 0; /* whole polygon is below horizon */

    /* make exponent odd */
    if ((e & 1) == 0) e = e+1;

    /* loop through edges of polygonal light source */
    i1 = j;
    for (i = 0; i < nv; i++) {

        /* next edge to process goes from v[(i+j)%nv] to v[(i+j+1)%nv] */
        i1++;
        if (i1 >= nv) i1 = 0;

        /* compute next vertex */
        diff_vector(v[i1],p,ui1);
        belowi1 = (dot(ui1,n) < 0);
        if (!belowi1) {
            COPY3(vi1,ui1);
            normalize(vi1);
        }

        if (belowi0 && !belowi1) {
            double vinter[3];
            /* edge arises from horizon */

            /* find intersection with horizon */
            seg_plane_intersection(ui0,ui1,n,vinter);
            normalize(vinter);

            /* add contribution from last vertex to intersection */

            /* don't need to add for exponents > 1 since
            contribution is 0 on boundary for such exponents */

            sum += shd_edge_contribution(vi0,vinter,n,1);

            COPY3(vi0,vinter);
        }
    }
}

```

```

} else if (!belowi0 && belowi1) {
    /* edge dives below horizon */

    /* find intersection wth horizon */
    seg_plane_intersection(ui0,ui1,n,vil);
    normalize(vil);
}

/* compute contribution from edge */
if (!belowi0 || !belowi1) sum += shd_edge_contribution(vi0,vil,n,e);

/* set next iteration's starting vertex to this iteration's ending vertex */
COPY3(ui0,ui1);
COPY3(vi0,vil);
belowi0 = belowi1;
}

if (sum < 0) sum = -sum; /* integrate around boundary in the right direction.
                          If negative, it was wrong. */
return sum/(2*M_PI);
}

```